Aerosol control on depth of warm rain in convective clouds

Mahen Konwar[1], R.S. Maheskumar[1], J. R. Kulkarni[1], E. Freud[2], B. N. Goswami[1] and D. Rosenfeld[2]

[1] Indian Institute of Tropical Meteorology, Pune, India 411 008

[2] The Hebrew University of Jerusalem, Jerusalem, Israel 91904

For correspondence:

mkonwar@tropmet.res.in

Contact: +91-9011050789

Abstract

Aircraft measurements of cloud condensation nuclei (CCN) and microphysics of clouds at various altitudes were conducted over India during CAIPEEX (Cloud Aerosol Interaction and Precipitation Enhancement Experiment) phase I and II in 2009 and 2010 respectively. As expected, greater CCN concentrations gave rise to clouds with smaller drops with greater number concentrations (N_c). The cloud drop effective radius (r_e) increased with distance above cloud base (D). Warm rain became detectable at the tops of growing convective clouds when r_e exceeded 12 μm with appreciable liquid water content (> 0.01 g/Kg). The r_e is determined by the number of activated CCN, N_{ad}, and D. The N_{ad} can be approximated by the maximum measured values of N_c. Higher N_c resulted in greater D for reaching the r_e threshold for onset of warm rain, r_e*, denoted as D*. In extreme cases of highly polluted and moist air that formed the monsoon clouds over the Indo-Gangetic plains, D* exceeded 6 km, well above the 0°C isotherm level. The precipitation particles were initiated there as supercooled rain drops at a temperature of -8°C. Giant CCN reduced r_e* and D*, by initiating raindrops at warmer temperatures. This effect was found mainly in dusty air masses over the Arabian Sea. Besides, the aerosol effect on D^*, D^* was found to decrease with increase in cloud water path.

1. Introduction

Anthropogenic cloud condensation nuclei (CCN) play a major role in determining cloud drop size distribution and precipitation forming processes. Much of the rainfall from convective clouds is initiated by drop coalescence. Clouds that form in air masses with higher CCN concentrations are composed of smaller droplets that are inefficient to coalesce into rain drops. Therefore, large concentrations of CCN (excluding giant CCN) suppress the formation of warm rain [*Gunn and Phillips*, 1957; *Twomey*, 1977; *Albrecht*, 1989; *Rosenfeld*, 2000; *Jayaraman*, 2001; *Ramanathan et al.*, 2001; *Hudson and Yum*, 2001; *McFarquhar and Heimsfield,* 2001; *Yum and Hudson*, 2002; *Rosenfeld et al.*, 2001; *Hudson and Mishra*, 2007; *Freud et al.*, 2008; *Hudson et al.*, 2009]. Rainfall would be suppressed from clouds that do not grow to sufficient depth for warm rain initiation, but this does not necessarily decrease the rainfall amounts from much deeper clouds. This is because suppression of warm rain due to higher CCN concentrations can invigorate convection by releasing latent heat in the conversion from liquid to ice phase cloud particles; this can further increase cloud depth and cloud lifetime, and eventually may result in more precipitation [*Andreae et al.*, 2004; *Khain et al.*, 2005; *Rosenfeld et al.*, 2008; *Li et al.*, 2011]. Giant CCN (GCCN) particles of diameter >1 µm condense to form large cloud drops, that more easily coalesce with the smaller drops to become rain drops [*Johnson*, 1982; *Beard and Ochs*, 1993; *Yin et al.*, 2000; *Rosenfeld et al.*, 2002; *Segal et al.*, 2004]. Thus, the GCCNs have the opposite effect to that of the small CCN particles on the onset of warm rain [*Hudson et al.* 2009; *Arthur et al.*, 2010; *Reiche and Lasher-Trapp*, 2010; *Hudson et al.,* 2011a]. Recent study by Gerber and Frick [2012] shows that GCCN significantly enhance rain in cumulus clouds only when cloud droplet concentration near its base N_c is rather large, but GCCN have very little effect on rain in clouds developing in pristine air. The altitude above cloud base (D) at which warm rain initiates in convective clouds is defined here as the depth for warm rain (D^*). D is the clouds depth i.e. distance from the clouds base. Larger concentrations of CCN increase D^*, whereas larger concentrations of GCCN decrease D^*. Therefore, it is important to quantify the interplay between CCN and GCCN on D^* and to establish the relationship of aerosol microphysical effects on clouds.

Theoretical studies show that the collision efficiencies of cloud droplets increase when the drop radius reaches 10 μm [*Pruppacher and Klett*, 1997]. Cloud drop effective radius (r_e) and its variation in convective clouds along the vertical dimension, has been shown to possess information about precipitation forming processes [*Rosenfeld and Lensky*, 1998]. r_e is defined as

$$r_e = \frac{\int N(r)\, r^3 dr}{\int N(r)\, r^2 dr} \tag{1}$$

where N and r are droplet concentration and radii, respectively. Greater D usually results in larger r_e. At sufficiently large D (i.e. D*) $r_e = r_e^*$, which is the threshold for precipitation onset according to aircraft measurements by *Gerber* [1996], who found r_e^* to be 14 μm in marine stratocumulus. *Rosenfeld and Gutman* [1994] combined satellite retrieved r_e and surface radar measurements to show r_e^* of 12 to 14 μm. This was subsequently reproduced by the Tropical Rainfall Measurement Mission (TRMM) satellite [*Rosenfeld*, 1999, 2000; *Rosenfeld et al.*, 2001; *Rosenfeld and Woodley*, 2003]. *Lensky and Drori* [2007] used a value of r_e^* = 15 μm for satellite delineation of precipitating clouds. Aircraft observations in the Amazon have shown that the cloud drops form warm rain when the modal diameter of the cloud droplet mass spectrum exceeds diameter D_L = 24 μm [*Andreae et al.*, 2004]; D_L is the drop diameter of modal liquid water content. Recently, *Freud and Rosenfeld* [2012] and *Freud et al.* [2011] showed the theoretical basis for the existence of r_e^*, and for the nearly linear dependence of D^* on N_c. They showed that the fundamental reason for the relationship between D^* and N_{ad} (number of activated CCN into cloud drops) is the observation that r_e increases with D as occurs in adiabatic cloud parcels. Therefore, the adiabatic concentration of drops that are nucleated near cloud base and the adiabatic cloud water content, determine r_v, the median volume radius of the cloud drops. Due to the similar shape of the drop size distributions at different heights, there is a very tight relationship between r_v and r_e. Therefore, r_e is determined to a close approximation by N_{ad} and D [*Freud et al.*, 2012]. The maximum N_c near cloud base is closely related to N_{ad}. Using aircraft measurements of convective clouds from very different climate regimes (including the data used in this study from 2009 during Cloud Aerosol Interaction and Precipitation Enhancement Experiment (CAIPEEX) phase I (hereafter CP–I) they showed that drizzle starts to form gradually in clouds with r_e>10 μm, but it accelerates rapidly to rain i.e., precipitation mass exceeding 0.03 g Kg^{-1} at r_e ~14 μm. Clouds over the Indian subcontinent are found to form few drizzle droplets when r_e is approximately 10 μm, but more significant drizzle occurs at r_e >12 μm with precipitation mass then exceeding 0.01 g Kg^{-1}. The rain rate increases sharply at r_e*=14 μm, at which precipitation mass exceeds 0.03 g kg^{-1} [*Konwar et al.*, 2010; *Freud and Rosenfeld*, 2011]. Here we show the relationships between CCN, D^* and r_e^* over India and its coastal waters.

Nearly 7.5 % of net Indian summer monsoon rainfall (ISMR) is due to heavy rainfall while 85% of net ISMR is due to low to medium rainfall. It is important to know how aerosol influences the convective precipitation processes albeit that the decadal ISMR trend is primarily governed by large scale dynamics and moisture inflow trends rather than aerosol trends [*Konwar* *et al.*, 2012a]. Since monsoon circulation is convectively coupled [*Goswami and Shukla*; 1984] understanding how aerosol and convective clouds interact is crucial. Aircraft observations of aerosol and clouds were obtained during the CP-I (May to September, 2009) and CAIPEEX phase II (CP-II) conducted from September to October, 2010 over the Indian subcontinent. Detail of CAIPEEX objectives, flight patterns and execution of the experiment during intense observation periods at different locations are discussed in *Kulkarni et al.* [2012]. The flight observations considered here were carried out at various environmental conditions over the Indian subcontinent e.g. over the Indo-Gangetic plain (IGP) in the north, Bay of Bengal (BoB) at the east coast, Arabian Sea (AS) at the west coast of the Indian peninsula and over some of the land masses in central, northeast and southern India. Details of the observational dates and places are provided in table I.

Here we utilize aircraft observations of CCN and cloud microphysical properties collected in extremely polluted conditions over IGP and pristine conditions over BoB during CP-I and CP-II. The objectives of this work are organized as follows:

1. The extent that the pollution aerosol can push upward D^* in convective clouds, as it determines the maximal depth of clouds in which air pollution can substantially suppress precipitation. Air pollution can possibly shut off precipitation completely from clouds with total cloud depth $<D^*$. This study explores the relationship between D^* and CCN measured right below cloud base.

2. How GCCN counteract the effect of small CCN in determining D^*. The interplay between CCN and GCCN on D^* is investigated and an empirical relationship is provided. Also the relationship between N_c and D^* is described.

2 Data Analysis

Details of flight mission objectives, methodologies of data analysis and quality control applied to the Cloud Droplet Probe (CDP), Cloud Image Probe (CIP) and CCN instrument can be found in *Kulkarni et al.* [2012]. It may be important to learn if there was any apparent drift in dT (temperature difference between the top and bottom of the column of the CCN counter) during CP-I and CP-II. The CCN counter was set at 0.2, 0.4 and 0.6 %SS during the campaign. The CCN counter was pre calibrated during CP-I while it was both pre and post calibrated during CP-II. The SS-dT relationship is provided in supplementary Fig. S1. There was little drift in SS, lesser than 4 to 7% of actual pre calibrated SS of 0.17 to 0.48%SS at different dT (see supplementary table-S1). As a result, for a given aerosol size distribution with 100% solubility, error in CCN measurement was within 5% of actual CCN count, which may be considered as insignificant (for details please see Fig. S2, table-S1 and supplementary material).

The cloud probes utilized in this campaign had round tip, the limitations of this type of tip are discussed in detail by *Korolev et al.* [2011]. Recent findings show that the shattering effect can cause artifacts of greater concentrations of small size ice hydrometeors when the CIP is exposed to mixed or ice phase hydrometeors [*Korolev et al.*, 2011]. However, these problems did not affect the present study, which is focused on warm rain. The CDP measures N_c of diameter 2.5 to 50 µm in 30 size bins while the Forward Scattering Spectrometer Probe (FSSP) measures N_c of diameter 2.5 to 47 µm in 30 size bins. During CP-II, the FSSP measured the cloud droplets.

3. Results

3.1 Cloud Droplet Size Distributions of convective clouds

Here, we analyzed in detail, the hydrometeor images recorded in young growing convective clouds from their base to their tops, and identified the altitude at which precipitation-sized particles were observed. We considered measurements of 25 growing convective clouds where warm rain was formed. These young convective towers were profiled vertically in 300-500 m steps, from cloud base up to cloud top or vice versa, to altitudes of 8 km. Only young developing convective clouds were selected for horizontal penetrations at 100-300 m below cloud top, so that the observed rain drops could not have fallen from much greater altitudes, but must have developed or formed within or close to the measured cloud volume. A schematic diagram illustrating the in-situ onset of warm rain process in convective cloud is shown conceptually in Figure 1. This figure also shows how D* was measured. We consider rain liquid water content (RLWC) of the liquid hydrometeors (diameter of 50-1550 μm) and r_e threshold as criteria for warm rain onset as measured by the CDP. For temperatures below 0°C only supercooled rain drops are considered. Drizzle drops, can initiate at r_e =11 but more so at r_e= 12 μm with a minimal initial amount of RLWC of 0.01 g/m^3. We conservatively used the following criteria for initiation of rain formation when the first appreciable drizzle drops are formed; i.e. RLWC> 0.01 g/m^3 and r_e^*>12 μm [*Konwar et al.*, 2010; *Freud and Rosenfeld*, 2012].

One of the major objectives of CAIPEEX was to study cloud microphysical properties in different environments over the Indian subcontinent. Large variability of aerosol optical depth is observed over the Indian subcontinent from MODIS satellite [*Prasad et al.*, 2004]. There is also large variability in CCN concentrations (N_{CCN}) and thermodynamic conditions over the Indian subcontinent, which would produce variability in cloud droplet size distributions, D^* and r_e^*. A tail of large drops that nucleate on GCCN can lead to earlier formation of rain drops [*Johnson*, 1982]. Examples of cloud droplet size distribution profiles over various land masses, AS and IGP are shown in Figure 2a-e. The growing convective elements were horizontally penetrated either from cloud base to the aircraft ceiling height, which is 8 km or vice versa. Two cases of inland cloud observations over Raichur and East of Bangalore are shown in Figure 2a,b. Profiles of cloud drop size distributions (DSDs) for two successive days on 24 August and 25 August 2009 are presented in Figure 2c,d. Cloud DSDs over the AS are shown in Figure 2e. The threshold of modal cloud drop liquid water content of D_L = 24μm for warm rain formation as found by *Andreae et al.*, [2004] for the Amazon is shown on each panel by a solid vertical line. It is important to note that the DSDs can be different on different days, and even on successive days at the same location depending on the meteorological conditions. Westerly winds prevailed over Bareilly in IGP on 24/08/2009 while easterly winds prevailed on 25/08/2009 on successive days (not shown here). Larger tails of large droplets was observed at cloud base on 24/08/2009 over IGP while on 25/08/2009 narrower DSDs at the cloud base were observed; D^* for these successive days were 5.98 and 5.30 km respectively (see table I). The N_{CCN} at the cloud base was more when westerly wind prevailed compared to easterly wind on these two successive days i.e. on 24/08/2009 and 25/08/2009 respectively, suggesting the important role played by wind direction in modulating the cloud properties. Very hazy atmosphere with poor visibility was observed over the IGP regions. Ample monsoon rain resulted in flooding over the IGP region during the observational days which also added to the increase in moisture level. Studies by *Dey et al.* [2004] suggested that aerosol distribution over IGP is bimodal but due to the increase in coarse mode aerosol, a third peak at 1 μm is obtained which may be due to the growth of dust particles at high relative humidity. The dust particles are transported from the middle-east and the Thar Desert in western India when westerly wind prevailed during the monsoon season. Chemical analysis of aerosol collected over IGP indicated increases in mineral dust during the monsoon season [*Ram et al.*, 2010]. Simulations carried out with NASA Global Modeling Initiative chemical transport model suggests that mineral dust through water absorption onto the surface of the particles can increase cloud droplet activation by enhancing its CCN activity [*Karydis et al.* 2011]. The cloud base DSDs over the AS on 5/7/2009 (Fig 2e) were characterized by a much larger tail than over the IGP on 25/8/2009 (Fig. 2c) period, this implies the presence of GCCNs in the boundary layer, which were probably due to desert dust and sea salt particles. The dust was transported from the Arabian Peninsula, and reduced the visibility over coastal waters off Mangalore to less than 5 km. DSDs grown in pristine conditions are shown in Fig 2f, where the cloud droplets grew faster and resulted in wide cloud droplet spectra just above cloud base. Such wide droplet spectra with different fall velocities favors collision, coalescence processes and early onset of warm rain.

3.2 Evolution of r_e with respect to T

The growth of r_e with respect to T is shown in Figure 3. Values of r_e^* at which onset of warm rain took place in the convective clouds are provided in table I. The effective radius, r_e increased with cloud depth at different rates for these different locations. Even over IGP on 24/08/2009 and 25/08/2009 the characteristics of r_e-T profiles are very different for successive days. The r_e grew fast by vapor condensation over AS and reached D^* of about 2.0 km cloud base. The air had many GCCN that formed large tail of large drops near cloud base, which accelerated the rain in this dusty air over the sea. Over the IGP, r_e grew more slowly. The cloud base heights of the monsoon clouds were low (see table 1) and varied from 0.5 to 2 km with warm cloud base temperatures. Clouds over the IGP had to grow deeper (D^* ~ 6.0 km) before precipitation-sized particles were first observed which is slightly below the cloud tops. Precipitation initiated as super cooled rain droplets formed at ~ -8˚C over IGP regions. In contrast, over the AS, with only slightly lower cloud bases, warm rain formed at a temperature of 8˚C. In the convective clouds with higher cloud bases (~2.0 km) over land precipitation was initiated as supercooled rain at around -5˚C (see table I). For clouds grown in the most pristine air over BoB, cloud droplets grew larger so that D* was only 0.40 km. The clouds over the BoB were found to precipitate at a relatively warmer temperature primarily due to being grown in pristine conditions.

Clouds over Silchar and Khasi Hills, which are located near to the wettest place on Earth in Northeast India (NEI), formed warm rain at 4 to 5 °C (not shown here), which is a warmer temperature than clouds over central India or IGP. This was observed despite relatively high N_{CCN} over this region. The clouds over Silchar formed rain drops when r_e^* became ~15 µm. While at another location Nagaon in NEI, warm rain formed at T* -3 °C where r_e* was found to be ~14 µm (see table I). T* is the temperature for onset of warm rain. Supercooled rain prevailed well above the 0 °C isotherm level in these clouds. The reason for these differences in T* is mainly due to the differences in cloud base temperatures. *Freud and Rosenfeld* [2012] showed that r_e* is determined by N_{ad} and by the adiabatic cloud water. N_{ad} is determined by the CCN spectra and cloud base updraft. The adiabatic water is determined by cloud base temperature and pressure. The existence of T* near or below 0°C for most of the continental clouds grown in the polluted conditions, even when cloud base temperature is quite high (well above 20°C, see table

I), means that much of the precipitation over the Indian subcontinent was initiated as supercooled rain.

3.3 Control of CCN and GCCN on Warm Rain Depth

Initiation of precipitation may also be triggered by cold processes [e.g., *Lamb et al.*, 1981], but here we limit our study to the warm rain process where precipitation was initiated as rain drops, even when $T^*<0°C$, where rain initiates as supercooled water. We investigated here relationship between the N_{CCN} at 0.4% SS ($N_{0.4\%}$) below the cloud base and N_c above cloud base. $N_{0.4\%}$ were found after establishing the CCN-SS relations of the form $CCN=c\ SS^k$, just below the bases of the convective clouds (see table I). The values of the power 'k' are relatively high over the land, which are typical of continental environment [see table 9.2 in *Pruppacher and Klett*, 1997; *Cohard et al.*, 1998]. Relatively smaller values of 'k' obtained over AS and BoB indicate maritime air mass, consistent with 'k' values reported elsewhere [see table 9.1 in *Pruppacher and Klett*, 1997]. The means of the few largest cloud droplets concentrations (i.e. within 2% of the maximum N_c) at D of 0-4 km of the convective clouds were determined. The maximum Nc in the convective clouds was not always near cloud base but was often found at greater D. This is attributed mostly to the fact that the clouds grow taller above the bases that formed in the strongest updrafts where N_{ad} is greatest. Maximum N_c was probably not due to secondary nucleation [*Pinsky and Khain*, 2002], at least not in the polluted cases with relatively high cloud base and strong cloud base updrafts. Scatter plot for $N_{0.4\%}$ vs N_c is shown in figure 4. The N_c do not increase linearly with increase in the N_{CCN}. A power law of the form $N_c = a\ N_{CCN}^b$ is assumed between them, where 'a' is the coefficient and 'b' is the exponent to be determined. The relationship of $N_c = 21.57\ N_{CCN}^{0.44}$ was obtained at 95% confidence level with correlation coefficient R of 0.84. This means that the CCNs do not nucleate into cloud droplets linearly i.e. there is a decrease in the ratio of $N_c/N_{0.4\%}$ at higher N_{CCN}. The non linearity between the N_{CCN} and N_c , which was predicted by *Twomey* [1959], is due to the greater competition for available moisture at higher N_c due to higher N_{CCN} which thus lowers the SS. The SS is reduced by the greater surface area of the larger number of growing droplets when N_{CCN} is higher [*Hudson et al.*, 2010]. At higher N_{CCN}, N_c was closer to N_{CCN} at lower SS while at lower N_{CCN}, N_c was closer to N_{CCN} at higher SS. *Hudson et al.* [1984] suggested that effective SS occurs at the SS where N_{CCN} equals N_c.

Figure 5a,b shows control of $N_{0.4\%}$ and GCCN on D^*. Increase in concentrations of small CCN at cloud base increased D^* (Fig. 5a). Since D^* has a linear relationship with N_c (discussed in section 3.4) and N_c is non linearly related with N_{CCN}, D^* is found to have non linear relationship with N_{CCN}. D^* has a sound correlation of 0.73 with N_{CCN}. A power law of the form $D^*=0.31\ N_{CCN}^{0.31}$ was found between them. As discussed in the introduction, greater GCCN concentrations induce earlier precipitation. The GCCN produce large cloud droplets that can exceed a diameter of 30 μm at small D, in both continental and maritime conditions. The observed large cloud drops near cloud base can be used for inferring the GCCN concentrations [*Hudson and Yum*; 2001]. The combination of Passive Cavity Aerosol Spectrometer (PCASP)-CDP and PCASP-FSSP measurement below cloud base, were used to estimate giant and ultragiant particle concentrations, which probably resulted in broad cloud base DSDs over AS [*Konwar et al.*; 2012b]. In this study, the role of GCCN was inferred by the mass normalized reflectivity (m_6m_3) of the cloud droplet spectrum at the base,

$$\frac{m_6}{m_3} = \frac{\int N(D)\, D^6 dD}{\int N(D)\, D^3 dD} \qquad (2)$$

where m_6 is the sixth and m_3 is the third moment of DSDs. Large mass normalized reflectivity indicates the impact of GCCN that nucleated at the cloud base . The extended tail in Fig. 2e indicates the effect of GCCN on cloud base DSD. A scatter plot between GCCN and D^* is shown in Figure 5b. A weak negative correlation of R=-0.24 is found between GCCN and D^*. This means that the effect of CCN in pushing D^* to greater values is counteracted by the GCCN, which results in smaller D^*. The effect of GCCN was quite significant at very high N_{CCN} (polluted aerosol) over IGP (Fig. 5b). In relatively less polluted air masses with lower N_{CCN}, the already low D^* does not leave much room for the effect of GCCN of further lowering D^*.

The interplay between CCN and GCCN on D^* is illustrated in greater detail in Figure 6 where it can be seen that with increase in N_{CCN}, D^* clearly increases. With increase in GCCN, as represented by an increase in the mass normalized reflectivity, at the same NCCN, D^* mostly becomes smaller. However, the importance of GCCN was more significantly realized over the marine polluted environment of the AS, where warm rain formed at 8˚C. It is to be noted here that this figure consists of convective clouds that occurred in conditions from pristine to polluted. Convective clouds grew over the IGP region formed supercooled water at -8 ˚C found to be influenced by GCCN, though less substantially. It may be noted that during break or weak monsoon conditions over Indian subcontinent, high CCN concentrations can shut off warm rain, instead initiate mixed phase precipitation [Konwar et al., *2010*]. From regression relations between D^*, $CCN_{0.4\%\ SS}$ and m_6m_3, the empirical relation is found to be of the form,

$$D^* = 2.43 * \log_{10} N_{0.4\%} - 1.33 * \log_{10} m_6m_3 \qquad (3)$$

The relationship between D^* and $N_{0.4\%}$ and m_6m_3 are significant at 95% confidence level. The scatter plot between the estimated and observed D^* is shown in Figure 7. Correlation coefficient of 0.86 exists between them with mean square error of 0.74 km. A practical implication of this relation is that given $N_{0.4\%}$ and m_6 m_3 at the cloud base it may be possible to estimate D^*.

Besides the aerosol effect on the onset of warm rain, updraft and mixing also have an important role. The cloud parcels are subjected to velocity fluctuations and mixings due to the presence of turbulence [*Beard and Ochs*, 1993]. Other than CCN, different cloud base updraft velocity and temperature could also lead to different supersaturation maximum, which could produce different N_c. In this study we have shown the important role played by CCNs in delaying the warm rain process and GCCN's counteracting the effect of CCN to reduce the warm rain depth.

The above observational evidence indicates that higher N_{CCN} increases D^* while higher GCCN concentrations counteract it by reducing D^*. During the monsoon season, the Indian subcontinent receives moisture due to the strong westerly and, southwesterly wind from the AS and southerly wind from the BoB. We investigated whether, D^* has a relationship with the liquid cloud water path CWP (g/m^2), which is the amount of column cloud water obtained from Terra Moderate Resolution Imaging Spectroradiometer (MODIS) [*King et al.,* 1992]. For this, we considered the closest satellite measured CWP to areas over which the convective clouds were measured (table I). A weak relationship exists between D^* and CWP i.e. D^*=3.66 - 0.0032 CWP, with R = -0.19 and significant at 65% confidence level, indicates that with increase in cloud water availability in the atmosphere D^* decreases slightly. This relation is probably real, because theoretical considerations imply that because r_e at a given D should be larger for greater LWP with a given N_c [*Freud and Rosenfeld,* 2012]. It is found that CWP has no meaningful relationship with N_c or N_{CCN}. It is shown by *Li et al.* [2011] for, the Southern Great Plains site in the USA, that N_{CCN} has a weak relationship with wind speed and shear but no significant relationship with other meteorological parameters such as temperature profiles, dew point temperature, pressure, or humidity. The generation of GCCNs from the sea surface however increases with the increasing low level wind speed [*Colón-Robles et al.*, 2006; *Hudson et al.*, 2011b].

3.4 Influence of Cloud drop Number concentrations on Warm Rain Depth

In the last sections, it was shown that with increase in N_{CCN} the N_c also increased (see figure 4). Since N_c increases with N_{CCN} and in turn D^* also becomes larger, it is important to know the direct relationship between D^* and N_c. *Freud and Rosenfeld* [2012] have shown based on fundamental theoretical considerations that N_{ad} and D^* must be nearly linearly related to each other. Because N_{ad} and N_c are linearly related, especially at lower N_{CCN}, D^* should increase nearly linearly with N_c. This can be qualitatively explained by the fact that there is an inverse relationship between N_c and r_e for a given cloud depth. Therefore, larger N_c should induce greater D^*. The scatter plot between N_c and D^* is shown in figure 8. A correlation coefficient of 0.79 was found between N_c and D^*. Linear fit between N_c and D^* above 99.95% confidence level yield the relationship of D^*=0.0035 N_c +1.2 (indicated by solid line in figure 8).

4. Discussion and Summary

This work studies the microphysical effect of aerosol on tropical convective cloud developed in both pristine and polluted conditions over the Indian subcontinent. These cloud microphysical data were collected over the Indian subcontinent in 2009 and 2010 through the CAIPEEX experiment. Based on the effective radius (r_e>12 μm) and RLWC (>0.01 gm/cm^3) at which collision efficiency increases sufficiently to form warm rain at the tops of growing convective towers, the influence of aerosol on the depth of warm rain is studied. The relationship between warm rain depth D^*, CCN, GCCN and N_c are also shown. The important findings of this study are summarized as follows:

- The cloud droplet concentration increases non-linearly with the increase in N_{CCN} which is in agreement with the finding of Twomey [1959] that may be attributed to the decrease in SS as the CCN compete for the available moisture in the cloud parcel [*Hudson et al.*, 2010]. At higher N_{CCN}, N_c was closer to N_{CCN} at lower SS while at lower N_{CCN}, N_c was closer to N_{CCN} at higher SS

- Increasing concentrations of CCN push depth for warm rain to greater heights non-linearly in the convective clouds. In extreme polluted cases D^* exceeds 6 km. In the most pristine case found over BoB rain initiates at a very shallow cloud depth of 0.40 km. This result is consistent with the theoretical result that aerosol pushes the depth for warm rain by *Freud and Rosenfeld* [2012].

- The GCCN were found to decrease the depth for warm rain, counteracting the effect of small CCN. However this effect was secondary to the effect of small CCN, The effect of GCCN was quite significant at very high N_{CCN} (polluted aerosol) over IGP. In the less polluted air masses with lower N_{CCN}, the already low D* does not leave much room for the effect of GCCN of further lowering D*. Recent study by *Karydis et al.* [2011] suggests that water coating on dust particles can enhance CCN activity. Over the AS where desert dust and sea salt are suspected to act as GCCN, the GCCNs are instrumental in forming rain particles at lower D*. The effect of GCCN found in this study is in agreement with *Hudson et al.* [2011a] and *Gerber and Frick* [2012].

- The depth for warm rain initiation increased linearly with the drop number concentrations (N_c) which again indicates that with increase in N_c the coalescence and collision efficiency decreases [*Gun and Phillips*, 1957] which is in agreement with the theoretical result of *Freud and Rosenfeld* [2012].

- In most of the continental clouds the pollution levels produced clouds with large drop number concentrations that caused the precipitation to be initiated above the 0°C isotherm level as supercooled rain drops. While for the convective clouds over the Arabian Sea and Bay of Bengal precipitation processes initiate at a very warm temperature, even at 25 ºC over the BoB.

- Besides the aerosol influence on D^* over the Indian subcontinent, the cloud water path (CWP) also plays a role. Though D^* and CWP have low anti-correlation between them, with increase in CWP the D^* is found to decrease. This suggests that with increasing moisture quantity the shallow convective clouds would precipitate earlier i.e. shallow D^*, which may play a role in the redistribution of precipitation from such clouds in a global warming scenario. For example, the observed increasing decadal trend of moisture content over AS to the west of 80 °E is expected to result in increasing r_e which in turn increases contribution from low to medium rainfall [*Konwar et al.*, 2012]. In contrast moisture content to the east of 80 °E is expected to decrease r_e and respectively decreases low to medium rainfall.

Acknowledgements

CAIPEEX is funded by Ministry of Earth Science, Govt. of India. The authors sincerely acknowledge the effort of CAIPEEX team members for successfully conducting the aircraft observations. Thanks to the pilots for safely maneuvering the aircraft into the convective clouds. Thanks to Drs. D. Axisa of The National Center for Atmospheric Research, USA, R. Burger and Prof. S. Piketh of Wits University, South Africa for their participation and data quality control in CAIPEEX phase II. There are large numbers of people involved directly or indirectly, in the successful campaign of CAIPEEX experiment, the authors are grateful to all. Thanks to the four anonymous reviewers for their comments and suggestions that improved the quality of the manuscript.

Reference

Albrecht, B. A.: Aerosols, cloud microphysics, and fractional cloudiness, Science, 245, 1227–1230, 1989.

Andreae, M. O., D. Rosenfeld, P. Artaxo, A. A. Costa, G. P. Frank, and K. M. Longo (2004), Smoking rain clouds over the Amazon, *Science*, 303(5662), 1337– 1342.

Arthur, D.K., S. Lasher-Trapp, A. Abdel-Haleem, N. Klosterman, and D.S. Ebert (2010), A new three-dimensional visualization system for combining aircraft and radar data and its application to RICO observations, *J. Atmos. & Ocean. Tech.*, *27*, 811-828, doi: 10.1175/2009JTecha1395.1.

Beard, K. V. and H. T. Ochs III (1993), Warm-Rain Initiation: An Overview of Microphysical Mechanisms, *Jour. Appl. Meteor.*, *32*, 608-625.

Cohard, Jean-Martial, Jean-Pierre Pinty and C. Bedos, (1998), Extending Twomey's analytical estimate of nucleated cloud droplet concentrations from CCN spectra, *Jour. Atmos. Sci.*, *55*, 3348-3357.

Colón-Robles Marilé, R. M. Rauber and J. B. Jensen, (2006), Influence of low-level wind speed on droplet spectra near cloud base in trade wind cumulus, *Geophys. Res. Let.*, Vol. 33, L20814, doi:10.1029/2006GL027487.

De, S., S. N. Tripathi, and R. P. Singh (2004), Influence of dust storms on the aerosol optical properties over the Indo-Gangetic basin, *Jour. Geophy. Res.*, *109*, D20211, doi:10.1029/2004JD004924, 2004.

Freud, E., D. Rosenfeld, M. O. Andreae, A. A. Costa, and P. Artaxo (2008), Robust relations between CCN and the vertical evolution of cloud drop size distribution in deep convective clouds, *Atmos. Chem. Phys., 8*, 1661-1675.

Freud E., D. Rosenfeld and J. R. Kulkarni (2011), Resolving both entrainment-mixing and number of activated CCN in deep convective clouds, Atmos. Chem. Phys., 11, 12887–12900.

Freud E. and D. Rosenfeld (2012), Linear relation between convective cloud drop number concentration and depth for rain initiation, *Jour. Geophy. Res.*, *Early online release.* www.agu.org/pubs/crossref/pip/2011JD016457.shtml.

Gerber H. (1996), Microphysics of marine stratocumulus clouds with two drizzle modes *J.*

Atmos. Sci., *53*, 1649– 1662.

Gerber H. and G. Frick (2012), Drizzle rates and large sea-salt nuclei in small cumulus, *Jour. Geophy. Res.*, 117, doi:10.1029/2011JD016249.

Goswami B. N. and J. Shukla, (1984), Quasi-periodic oscillations in a symmetric general circulation model. *J. Atmos. Sci.*, 41**,** 20–37.

Gun, R. and B. B. Phillips (1957), A experimental investigation of the effect of air pollution on the initiation of rain, *Jour. of Meteor.*, *14*, 272-280.

Hudson, J. G., and S. S. Yum (2001), Maritime-continental drizzle contrasts in small cumuli, *J. Atmos. Sci.*, *58*, 915–926.

Hudson, J. G. (1984), CCN measurements within clouds, *J. Clim. Appl. Meteorol.*, 23,42-51.

Hudson, J. G., and S. Mishra (2007), Relationships between CCN and cloud microphysics variations in clean maritime air, *Geophys. Res. Lett.*, *34*, L16804, doi:10.1029/2007GL030044.

Hudson, J. G., S. Noble, V. Jha, and S. Mishra (2009), Correlations of small cumuli droplet and drizzle drop concentrations with cloud condensation nuclei concentrations, *J. Geophys. Res.*, *114*, D05201, doi:10.1029/2008JD010581.

Hudson, J.G., V. Jha, and S. Noble, (2011a) Drizzle correlations with giant nuclei. *Geophys. Res. Lett.* http://www.agu.org/journals/gl/papersinpress.shtml#id2010GL046207 .

Hudson, J.G., S. Noble, and V. Jha (2011b) On the relative role of sea salt cloud condensation nuclei (CCN), *J. Atmos. Chem.*, DOI: 10.1007/s10874-011-9210-5.

Jayaraman, A. (2001), Aerosol radiation cloud interactions over the tropical Indian Ocean prior to the onset of the summer monsoon, *Curr. Sci.*, *81*, 1437-1445.

Johnson, D. B. (1982), The role of giant and ultragiant aerosol particles in warm rain initiation, *Jour. Atmos. Sci.*, *39*, 448-460.

Karydis, V. A., P. Kumar, D. Barahona, I. N. Sokolik and A. Nenes (2011), On the effect of dust particles on global cloud condensation nuclei and cloud droplet number, *J. Geophys. Res*, *116,* D23204, doi:10.1029/2011JD016283.

Khain, A., D. Rosenfeld, and A. Pokrovsky (2005), Aerosol impact on the dynamics and microphysics of deep convective clouds, *Quart. Journ. of Royal Meteor. Soc.*, *131*, 2639–2663.

King, M. D., Y. J. Kaufman, W. P. Menzel, and D. Tané (1992), Remote sensing of cloud, aerosol, and water vapor properties from Moderate Resolution Imaging Spectrometer (MODIS). *IEEE Trans. Geosc and Rem Sen.*,*30*, 2-27.

Konwar, M., R. S. Maheskumar, J. R. Kulkarni, E. Freud, B. N. Goswami, and D. Rosenfeld (2010), Suppression of warm rain by aerosols in rain-shadow areas of India, *Atmos. Chem. Phys. Discuss.*, *10*, 17009-17027.

Konwar, M., A. Parekh and B. N. Goswami (2012a), Dynamics of East-West Asymmetry of Indian Summer Monsoon Rainfall Trends in Recent Decades, *Geophys. Res. Lett.*, doi:10.1029/2012GL052018. .

Konwar, M., R. S. Maheshkumar, J.R. Kulkarni, B. Padmakumari, S. B. Morwal, C. G. Deshpande, D. Axisa, R. Burger, S. Piketh, D. Rosenfeld and B. N. Goswami (2012b), Contrasting polluted and pristine cloud microphysical properties over the Arabian Sea and Bay of Bengal, presented in "Opportunities and Challenges in Monsoon Prediction in a Changing Climate" (OCHAMP-2012) held at IITM, Pune.

Korolev, V., E. F. Emery, J.W. Strapp, S. G. Cober, G. Isaac, M. Wasey, and D. Marcotte, Small ice particles in tropospheric clouds: fact or artifact? Airborne Icing Instrumentation Evaluation Experiment (2011), *Bull. American Meteor. Soc.*, doi:10.1175/2010BAMS3141.1.

Kulkarni J. R. and co-authors (2012), The Cloud Aerosol Interactions and Precipitation Enhancement Experiment (CAIPEEX): Overview and Preliminary Results, *Current Science*, 102, http://cs-test.ias.ac.in/cs/php/forthcoming/RA163.pdf.

Lamb D., J. Hallett and R. I. Sax (1981), Mechanistic limitations to the release of latent heat during the natural and artificial glaciations of deep convective clouds, Quart. J. R.Met. Soc. 107, 935-954.

Lensky, I. M., R. Drori (2007), A Satellite-Based Parameter to Monitor the Aerosol Impact on Convective Clouds, *J. Appl. Meteor. Climatol., 46*, 660–666.

Li, Z., F. Niu, J. Fan, Y. Liu, D. Rosenfeld and Y. Ding (2011), Long-term impacts of aerosols on the vertical developments of clouds and precipitation, *Nat. Geosci.*, doi:10.1038/NGEO1313.

McFarquhar, G. M., and A. J. Heymsfield (2001), Parameterizations of INDOEX microphysical measurements and calculations of cloud susceptibility: Applications for climate studies, *J. Geophys. Res.*, *106*, 28 675–28 698.

Pinsky, M. and A. P. Khain, 2002: Effects of in-cloud nucleation and turbulence on 34 droplet spectrum formation in cumulus clouds. *Quart. J. Roy. Meteorol. Soc.*, **128**, 35 1–33.

Prasad, A. K., R. P. Singh and A. Singh (2004), Variability of Aerosol Optical Depth Over Indian Subcontinent Using MODIS Data, *Jour. of Ind. Soc. of Remote Sensing*, 32(4).

Pruppacher, H. R., and J. D. Klett (1997), Microphysics of Clouds and Precipitation, Kluwer Academic Publ., 2nd Edition, 954pp.

Ramanathan, V., P. J. Crutzen, J. T. Kiehl, D. Rosenfeld (2001), Aerosol, Climate and Hydrological cycle, *Science*, *294*,2119-2124,.

Ramanathan, V., P. J. Crutzen, A. P. Mitra, and D. Sikka (2002), The Indian Ocean Experiment and The Asian Brown Cloud, *Curr. Sci.*, *83*, 947-955.

Ram, K., M. M. Sarin, and P. Hedge (2010), Long-term record of aerosol optical properties and chemical composition from a high-altitude site (Manora Peak) in Central Himalaya, *Atmos. Chem. Phys.*, *10*, 11791–11803.

Reiche C. H. and S. Lasher-Trapp (2010), The minor importance of giant aerosol to precipitation development within small trade wind cumuli observed during RICO, *Atmos. Res.*, *95*, 386–399.

Rosenfeld, D., and G. Gutman (1994), Retrieving microphysical properties near the tops of potential rain clouds by multispectral analysis of AVHRR data, *Atmo. Res.*, *34*, 259-283.

Rosenfeld D. (1999), TRMM Observed First Direct Evidence of Smoke from Forest Fires Inhibiting Rainfall, *Geophys. Res. Lett.*, *26(20)*, 3105–3108.

Rosenfeld, D. (2000), Suppression of rain and snow by urban and industrial air pollution, *Science*, *287*, 1793-1796.

Rosenfeld, D., Y. Rudich, and R. Lahav (2001), Desert dust suppressing precipitation: A possible desertification feedback loop, *Proc. Natl. Acad. Sci. USA*, *98*, 5975-5980.

Rosenfeld, D., R. Lahav, A. Khain, and M. Pinsky (2002), The role of sea spray in cleansing air pollution over ocean via cloud processes, *Science*, *297*, 1667–1670.

Rosenfeld, D., U. Lohmann, G. B. Raga, C. D. O´Dowd, M. Kulmala, S. Fuzzi, A. Reissell and M. O. Andrae (2008), Flood or Drought: How aerosols affect precipitation?, *Science*, *321*, 1309-1313.

Segal, Y., A. Khain, and M. Pinsky (2004), Effects of atmospheric aerosol on precipitation in cumulus clouds as seen from 2000-bin cloud parcel microphysical model: Sensitivity study with cloud seeding applications, *Q. J. R. Meteorol. Soc.*, *130*, 561–582.

Twomey, S. (1959), The supersaturation in natural clouds and the variation of cloud droplet Concentration, *Geofis. Pura appl*. *43*, 243-249.

Twomey, S. (1966), Computations of Rain formation by coalescence, *Journ. Atmos. Sci.*, *23*, 405-411.

Twomey, S. (1977), *Atmospheric Aerosols*, 302 pp., Elsevier Sci., New York.

Yin, Y., Z. Levin, T. G. Reisin, and S. Tzivion (2000), The effects of giant cloud condensational nuclei on the development of precipitation in convective clouds: A numerical study, *Atmos. Res.*, *53*, 91–116.

Yum, S. S., and J. G. Hudson (2002), Maritime/continental microphysical contrasts in stratus, *Tellus, Ser. A and Ser. B*, *54B*, 61–73.

Table I: Observational dates and location, Time of flight in Indian Standard Time (UTC+5:30 hr), MODIS cloud water path CWP (g/m^2), Cloud base height Cb (km), Cloud base temperature (ºC) Mass Normalized Reflectivity m_6m_3 (mm^3), Warm Rain Depth D* (km), effective radius r_e^* at D*, temperature T* at D* for the convective clouds, maximum cloud droplets N_c (cm^{-3}), CCN-SS relationships of the form CCN=cSS^k at cloud base as obtained from aircraft measurements during CAIPEEX phase I (2009) and phase II (2010). The SS was set at 0.2 %, 0.4 % and 0.6%. , c is the concentration at 1%SS.

Sl. No.	Date and Location	Time of flight (IST) ,Start Time-End Time	CWP g/m^2	Cb Km	T_{Cb} ºC	m6m3 mm^3	WRD D* km	r_e^* µm	T* °C	N_c cm^{-3}	CCN at 0.4%SS cm^{-3}	CCN=cSS^k c	K
1	22nd Jun, Raichur	13:15 - 16:15	43	2.02	15.50	795	3.25	14.97	-4.86	337	657	1939	1.18
2	27nd Jun, East-Bangalore	11:25 - 15:00	173	2.15	14.45	1423	4.28	13.94	-9.03	978	1769	1975	0.12
3	28th Jun, Western Ghat	12:25 - 15:40	150	1.90	17.62	2692	2.90	11.00	-1.00	870	2095	3665	0.61
4	05th Jul, AS	11:55 - 15:10	237	0.60	21.00	10659	1.92	13.50	11.79	433	884	1532	0.60
5	07th Jul, AS	11:40 - 15:20	240	0.68	20.17	6718	1.14	11.06	8.29	534	964	1672	0.60
6	13th Jul, AS	12:15 - 16:00	274	0.62	21.50	4174	1.90	10.59	11.4	508	1402	3412	0.97
7	13th Jul, Western Ghat	12:15 - 16:00	274	1.90	15.30	956	0.98	13.00	9.26	262	735	1080	0.42
8	14th Aug., Hyderabad	14:35 - 17:20	69	1.98	16.40	2340	4.08	11.77	-5.24	571	2446	10500	1.59
9	16th Aug., Hyderabad	14:35 - 16:40	121	1.44	18.80	1726	4.55	15.07	-6.24	600	2049	5667	1.11
10	18th Aug., IGP	13:00 - 16:15	121	1.00	23.80	5107	4.81	10.82	-2.06	1257	10635	27580	1.04
11	23th Aug.,IGP	14:15 - 17:00	69	1.17	22.12	3096	5.24	11.93	-7.23	994	7418	17080	0.92
12	24th Aug.,IGP	14:10 - 16:20	84	0.74	25.00	2237	5.98	12.57	-8.28	1090	8887	18840	0.82
13	25th Aug., IGP	14:15 - 16:15	219	0.65	24.50	1069	5.30	14.35	-6.56	875	3361	14300	1.58
14	30 Aug, Khasi Hills	14:45 - 17:00	165	0.90	20.00	1960	3.40	15.50	4.00	300	1153	1980	0.59
15	04th Sep Nagaon	12:45 - 16:05	253	1.08	24.00	1314	2.95	14.16	-3.00	575	2470	12391	1.76
16	04th Sep Silchar	12:45 - 16:05	211	1.48	20.75	1298	3.05	15.60	5.00	561	2434	7112	1.17
17	06th Sep Silchar	11:45 - 14:15	159	1.64	18.36	1654	2.97	15.90	4.30	350	1229	3131	1.02
18	28th Sep Visakhapattanam	13:35 - 17:40	323	0.76	20.85	917	4.61	13.20	-1.0	830	2731	10700	1.49
	CAIPEEX Phase II												
19	14 Sep, Raichur	13:00 - 15:18	101	1.00	23.00	772	3.00	11.00	9.55	336	316	558	0.62
20	16 Sep, Hyderabad	13:01 - 15:38	70	1.50	19.00	450	2.20	13.79	-6.0	361	288	645	0.88
22	23 Sep, Hyderabad	12:59 - 15:14	78	0.58	25.37	1006	1.95	15.50	15.00	210	306	593	0.72
23	26 Sep., BoB	11:27- 13:13	143	0.55	21.56	1448	1.78	11.00	17.00	110	174	308	0.62
24	27 Sep., BoB	11:36 - 13:30	65	0.60	25.77	4508	0.40	13.52	24.70	47	79	150	0.69
25	29 Oct., BoB	11:58-15:00	347	0.80	24.8	999	2.30	14.24	9.00	114	286	440	0.47

Figure Captions

Figure 1: A schematic diagram for a developing convective cloud with images of in situ hydrometeors at cloud top that represent the microphysical processes. The effective radius (r_e) is shown conceptually by the blue line, r_e reaches 12µm when precipitation is first seen at a cloud depth. When precipitation forms (RLWC> 0.01 g/m^3)the distance from cloud base to corresponding cloud depth is called the depth of warm rain, D^*.

Figure 2: Evolution of cloud droplets over (a) Raichur on 22/06/2009, adopted from *Konwar et al.* [2010], (b) East of Bangalore on 27/06/2009, over Bareilly in Indo-Gangatic Plan on (c) 24/08/2009 and (d) 25/08/2009, (e) over the Arabian Sea on 05/07/2009 and (f) over the Bay of Bengal on 27/09/2010. The vertical solid line indicates the modal LWC diameter of 24 µm for onset of warm rain (Andreae et al., 2004). The legend on each panel shows the UTC time in hour, minute and seconds of the cloud pass and altitude separated by a dot with corresponding DSD. The DSDs are the mean of instantaneous DSD per second collected within a cloud pass length considered for more than 3 sec. The DSD profiles show a nice evolution of the cloud droplet spectrum with altitudes though the convective clouds are turbulent in nature. Also note the cloud base DSD tails extended to larger drop diameters over Bareilly (panel c) when westerly wind prevailed and Arabian Sea (panel e) that signify the presence of giant CCN. Large cloud droplets at cloud base were absent when easterly wind prevailed over IGP (panel d)

Figure 3: Evolution of effective radius (r_e) vs T over Raichur, Bangalore, Indian Ocean off the coast of Mangalore, Indo-Gangatic Plains (IGP) and Bay of Bengal. The most polluted case is for IGP while most pristine is for BoB. The critical r_e at 12 µm for triggering drop coalescence and collision is shown by the solid line. The r_e at the Bay of Bengal case does not increase above 17 µm due to rainout (Rosenfeld and Lensky, 1998). The r_e-T relationship over Raichur on

22062009 is adopted from *Konwar et al.* [2010]. The altitude corresponding to T is provided in colorbar.

Figure 4: Relationship between CCN Concentrations at 0.4% Supersaturation ($N_{0.4\%}$) below cloud base and Cloud Droplet Concentrations (Nc) a few kilometers above cloud base of the convective clouds. A nonlinear fit of the form $Nc=21.63\ N_{0.4\%}^{0.44}$ is significant at 95% confidence level since relationship between them is non-linear [*Twomey* 1959].

Figure 5: (a) Cloud condenstion nuclei (CCN) control of the warm rain depth. Greater CCN concentrations increase the depth of warm rain D^*. (b) Giant CCN concentrations lower the warm rain depth, significant to 75% confidence level. The Giant CCN concentration is approximated by the ratio of sixth moment of cloud base DSD to third moment of cloud base DSD (mass normalized reflectivity, mm^3). Presence of GCCN is indicated by large value, of mass normalized reflectivity primarily due to long tail of cloud base DSD (see figure 2e).

Figure 6: Interplay between CCN at SS=0.4% and GCCN on the depth of warm rain. High CCN concentrations push the depth for warm rain higher (D^*) while GCCNs (large Mass Normalized DSDs) induce smaller D^*. For a given CCN, more GCCN (larger circle) show shallower depth for initiation of warm rain, D* .

Figure 7: Observed vs. estimated warm rain depth as obtained from multiple regression relation of CCN, m_6m_3 and D^*.

Figure 8: Relation between Cloud Droplet Concentrations (N_c) and Warm Rain Depth (D^*) with correlation coefficient of 0.79.

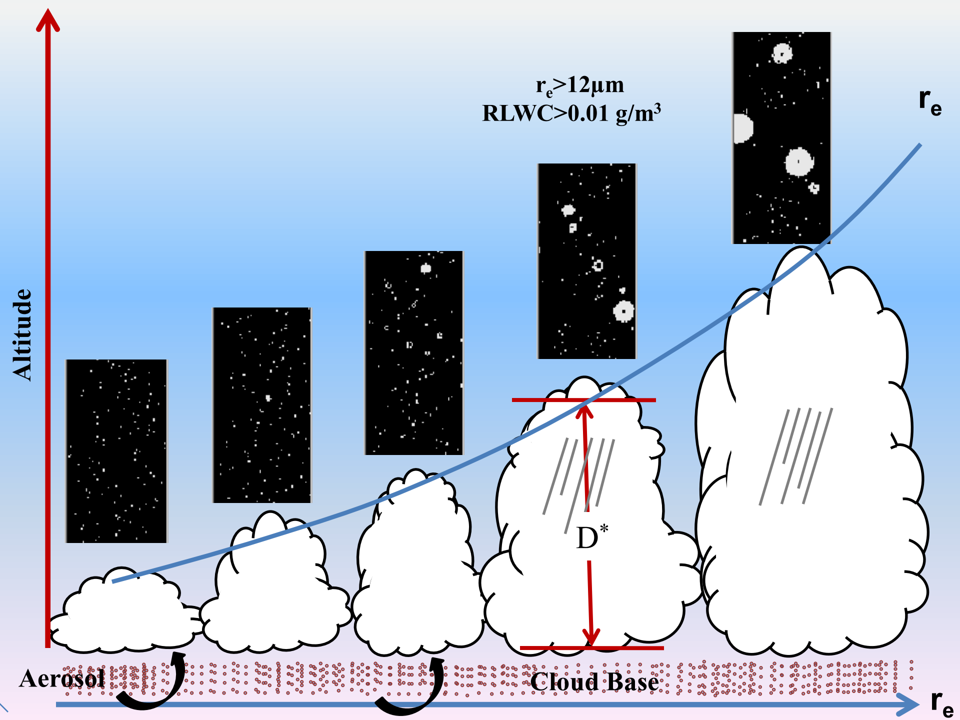

r_e>12μm
RLWC>0.01 g/m^3
r_e
Altitude
D^*
Aerosol
Cloud Base
r_e

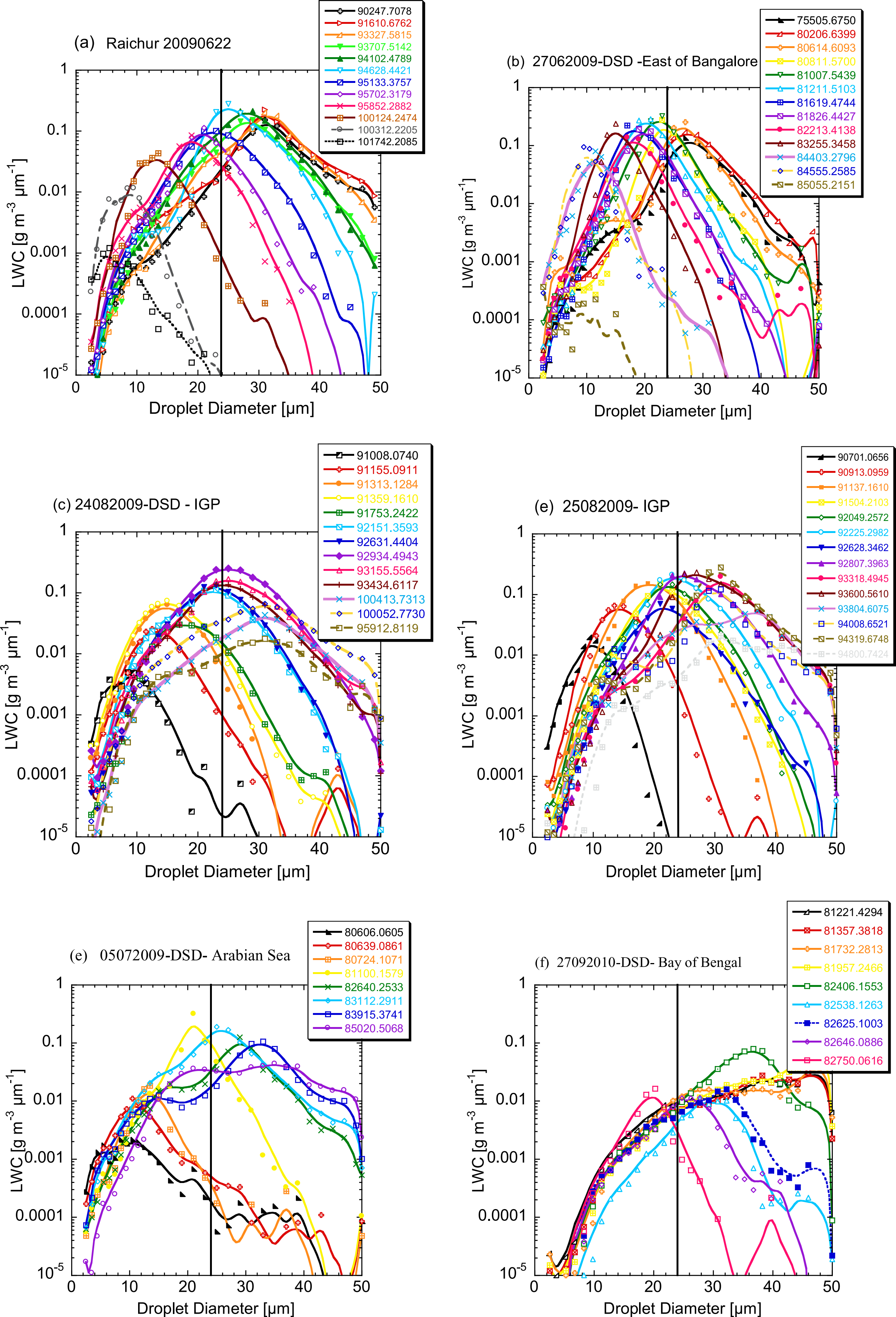
(a) Raichur 20090622
90247.7078
91610.6762
93327.5815
93707.5142
94102.4789
94628.4421
95133.3757
95702.3179
95852.2882
100124.2474
100312.2205
101742.2085
LWC [g m^-3 μm^-1]
Droplet Diameter [μm]
(b) 27062009-DSD -East of Bangalore
75505.6750
80206.6399
80614.6093
80811.5700
81007.5439
81211.5103
81619.4744
81826.4427
82213.4138
83255.3458
84403.2796
84555.2585
85055.2151
LWC [g m^-3 μm^-1]
Droplet Diameter [μm]
(c) 24082009-DSD - IGP
91008.0740
91155.0911
91313.1284
91359.1610
91753.2422
92151.3593
92631.4404
92934.4943
93155.5564
93434.6117
100413.7313
100052.7730
95912.8119
LWC [g m^-3 μm^-1]
Droplet Diameter [μm]
(e) 25082009- IGP
90701.0656
90913.0959
91137.1610
91504.2103
92049.2572
92225.2982
92628.3462
92807.3963
93318.4945
93600.5610
93804.6075
94008.6521
94319.6748
94800.7424
LWC [g m^-3 μm^-1]
Droplet Diameter [μm]
(e) 05072009-DSD- Arabian Sea
80606.0605
80639.0861
80724.1071
81100.1579
82640.2533
83112.2911
83915.3741
85020.5068
LWC [g m^-3 μm^-1]
Droplet Diameter [μm]
(f) 27092010-DSD- Bay of Bengal
81221.4294
81357.3818
81732.2813
81957.2466
82406.1553
82538.1263
82625.1003
82646.0886
82750.0616
LWC [g m^-3 μm^-1]
Droplet Diameter [μm]

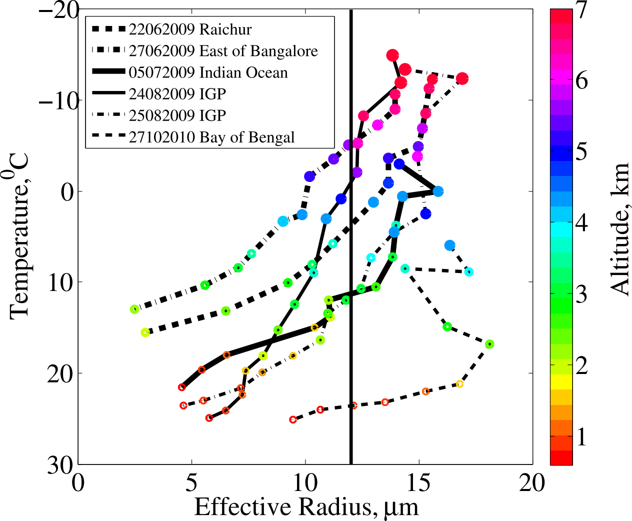
22062009 Raichur
27062009 East of Bangalore
05072009 Indian Ocean
24082009 IGP
25082009 IGP
27102010 Bay of Bengal
Temperature, ^{0}C
Effective Radius, μm
Altitude, km
−20
−10
0
10
20
30
0
5
10
15
20
1
2
3
4
5
6
7

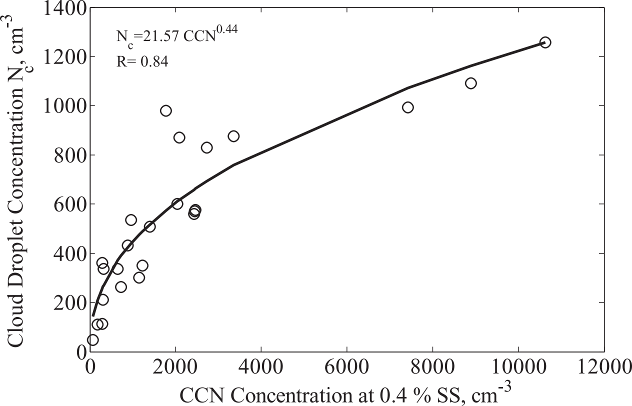

N_c=21.57 $CCN^{0.44}$
R= 0.84
Cloud Droplet Concentration N_c, cm^{-3}
CCN Concentration at 0.4 % SS, cm^{-3}
0
200
400
600
800
1000
1200
1400
0
2000
4000
6000
8000
10000
12000

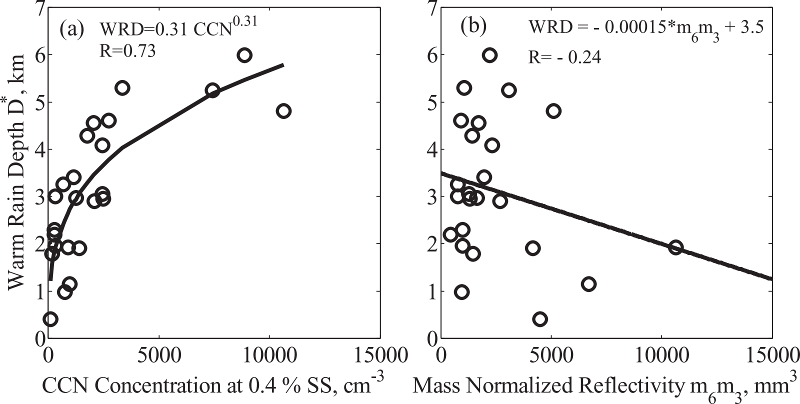

(a)
WRD=0.31 CCN$^{0.31}$
R=0.73
(b)
WRD = - 0.00015*m_6m_3 + 3.5
R= - 0.24
Warm Rain Depth D^*, km
CCN Concentration at 0.4 % SS, cm^{-3}
Mass Normalized Reflectivity m_6m_3, mm^3
0
1
2
3
4
5
6
7
5000
10000
15000

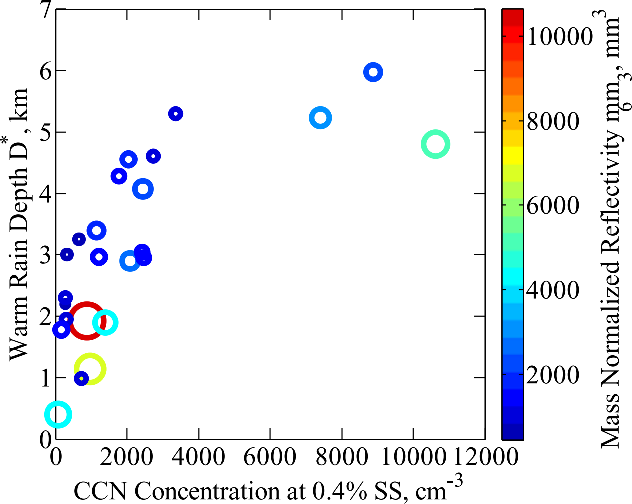

Warm Rain Depth D*, km
CCN Concentration at 0.4% SS, cm-3
Mass Normalized Reflectivity mm6, mm3
0
1
2
3
4
5
6
7
0
2000
4000
6000
8000
10000
12000
2000
4000
6000
8000
10000

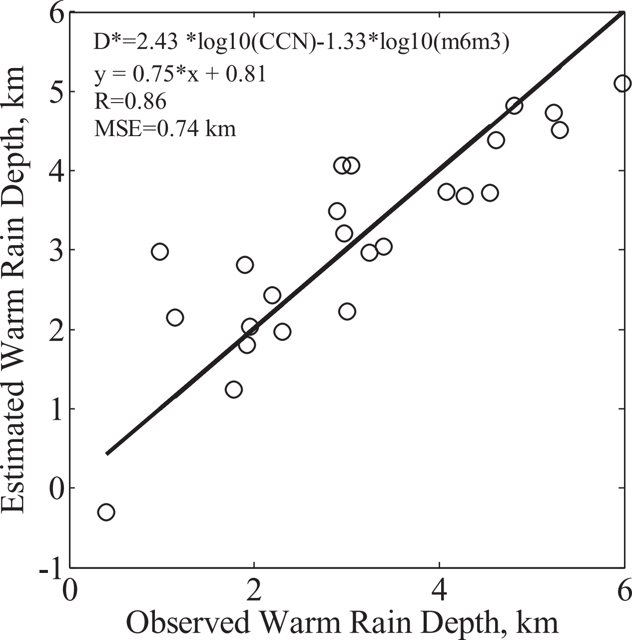

D*=2.43 *log10(CCN)-1.33*log10(m6m3)
y = 0.75*x + 0.81
R=0.86
MSE=0.74 km
Estimated Warm Rain Depth, km
Observed Warm Rain Depth, km
-1
0
1
2
3
4
5
6
0
2
4
6

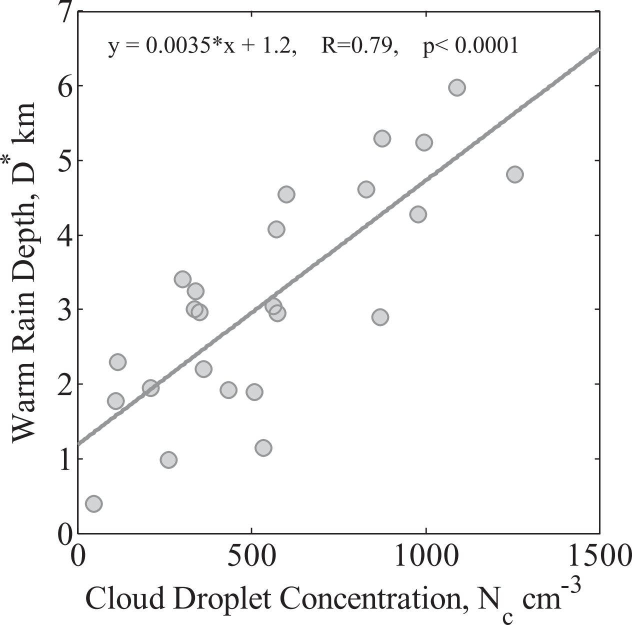
y = 0.0035*x + 1.2,   R=0.79,   p< 0.0001
Warm Rain Depth, D* km
Cloud Droplet Concentration, N_c cm^-3
0
1
2
3
4
5
6
7
0
500
1000
1500